β-Delayed One and Two Neutron Emission Probabilities Southeast of ^{132}Sn and the Odd-Even Systematics in r-Process Nuclide Abundances

V. H. Phong,[1,2,*] S. Nishimura,[1,†] G. Lorusso,[1,3,4] T. Davinson,[5] A. Estrade,[6] O. Hall,[5] T. Kawano,[7] J. Liu,[1,8] F. Montes,[9] N. Nishimura,[10,1] R. Grzywacz,[11] K. P. Rykaczewski,[12] J. Agramunt,[13] D. S. Ahn,[1,14] A. Algora,[13] J. M. Allmond,[12] H. Baba,[1] S. Bae,[14] N. T. Brewer,[12,11] C. G. Bruno,[5] R. Caballero-Folch,[15] F. Calviño,[16] P. J. Coleman-Smith,[17] G. Cortes,[16] I. Dillmann,[15,18] C. Domingo-Pardo,[13] A. Fijalkowska,[19] N. Fukuda,[1] S. Go,[1] C. J. Griffin,[5] J. Ha,[1,20] L. J. Harkness-Brennan,[21] T. Isobe,[1] D. Kahl,[5,22] L. H. Khiem,[23,24] G. G. Kiss,[1,25] A. Korgul,[19] S. Kubono,[1] M. Labiche,[17] I. Lazarus,[17] J. Liang,[26] Z. Liu,[27,28] K. Matsui,[1,29] K. Miernik,[19] B. Moon,[14] A. I. Morales,[13] P. Morrall,[17] N. Nepal,[6] R. D. Page,[21] M. Piersa-Siłkowska,[19] V. F. E. Pucknell,[17] B. C. Rasco,[12] B. Rubio,[13] H. Sakurai,[1,29] Y. Shimizu,[1] D. W. Stracener,[12] T. Sumikama,[1] H. Suzuki,[1] J. L. Tain,[13] H. Takeda,[1] A. Tarifeño-Saldivia,[16,13] A. Tolosa-Delgado,[13] M. Wolińska-Cichocka,[30] P. J. Woods,[5] and R. Yokoyama[11,31]

[1]*RIKEN Nishina Center, Wako, Saitama 351-0198, Japan*
[2]*University of Science, Vietnam National University, Hanoi 120062, Vietnam*
[3]*National Physical Laboratory, Teddington TW11 0LW, United Kingdom*
[4]*Department of Physics, University of Surrey, Guildford GU2 7XH, United Kingdom*
[5]*School of Physics and Astronomy, University of Edinburgh, Edinburgh EH9 3FD, United Kingdom*
[6]*Department of Physics, Central Michigan University, Mount Pleasant, Michigan 48859, USA*
[7]*Theoretical Division, Los Alamos National Laboratory, Los Alamos, New Mexico 87545, USA*
[8]*Department of Physics, University of Hong Kong, Pokfulman Road, Hong Kong*
[9]*National Superconducting Cyclotron Laboratory, East Lansing, Michigan 48824, USA*
[10]*Astrophysical Big-Bang Laboratory, Cluster for Pioneering Research, RIKEN, Wako, Saitama 351-0198, Japan*
[11]*Department of Physics and Astronomy, University of Tennessee, Knoxville, Tennessee 37996, USA*
[12]*Physics Division, Oak Ridge National Laboratory, Oak Ridge, Tennessee 37831, USA*
[13]*Instituto de Fsica Corpuscular, CSIC and Universitat de Valencia, E-46980 Paterna, Spain*
[14]*Center for Exotic Nuclear Studies, Institute for Basic Science, Daejeon 34126, Republic of Korea*
[15]*TRIUMF, Vancouver, British Columbia V6T 2A3, Canada*
[16]*Universitat Politecnica de Catalunya, E-08028 Barcelona, Spain*
[17]*STFC Daresbury Laboratory, Daresbury, Warrington WA4 4AD, United Kingdom*
[18]*Department of Physics and Astronomy, University of Victoria, Victoria, British Columbia V8P 5C2, Canada*
[19]*Faculty of Physics, University of Warsaw, PL02-093 Warsaw, Poland*
[20]*Seoul National University, Department of Physics and Astronomy, Seoul 08826, Republic of Korea*
[21]*Department of Physics, University of Liverpool, Liverpool L69 7ZE, United Kingdom*
[22]*Extreme Light Infrastructure—Nuclear Physics, Horia Hulubei National Institute for R&D in Physics and Nuclear Engineering (IFIN-HH), 077125 Bucharest-Măgurele, Romania*
[23]*Institute of Physics, Vietnam Academy of Science and Technology, Ba Dinh, 118011 Hanoi, Vietnam*
[24]*Graduate University of Science and Technology, Vietnam Academy of Science and Technology, Cau Giay, 122102 Hanoi, Vietnam*
[25]*Institute for Nuclear Research (Atomki), Debrecen H4032, Hungary*
[26]*McMaster University, Department of Physics and Astronomy, Hamilton, Ontario L8S 4M1, Canada*
[27]*Institute of Modern Physics, Chinese Academy of Sciences, Lanzhou 730000, China*
[28]*School of Nuclear Science and Technology, University of Chinese Academy of Sciences, Beijing 100049, China*
[29]*University of Tokyo, Department of Physics, Tokyo 113-0033, Japan*
[30]*Heavy Ion Laboratory, University of Warsaw, Pasteura 5A, PL-02-093 Warsaw, Poland*
[31]*Center for Nuclear Study, University of Tokyo, RIKEN Campus, 2-1 Hirosawa, Wako, Saitama 351-0198, Japan*

The β-delayed one- and two-neutron emission probabilities (P_{1n} and P_{2n}) of 20 neutron-rich nuclei with $N \geq 82$ have been measured at the RIBF facility of the RIKEN Nishina Center. P_{1n} of ^{130,131}Ag, ^{133,134}Cd, ^{135,136}In, and ^{138,139}Sn were determined for the first time, and stringent upper limits were placed on P_{2n} for nearly all cases. β-delayed two-neutron emission (β2n) was unambiguously identified in ^{133}Cd and ^{135,136}In, and their P_{2n} were measured. Weak β2n was also detected from ^{137,138}Sn. Our results highlight the effect of the $N = 82$ and $Z = 50$ shell closures on β-delayed neutron emission probability and provide stringent benchmarks for newly developed macroscopic-microscopic and self-consistent global models with the inclusion of a statistical treatment of neutron and γ emission. The impact of our measurements on r-process nucleosynthesis was studied in a neutron star merger scenario. Our P_{1n} and P_{2n} have a direct impact on the

odd-even staggering of the final abundance, improving the agreement between calculated and observed Solar System abundances. The odd isotope fraction of Ba in *r*-process-enhanced (*r*-II) stars is also better reproduced using our new data.

The nucleosynthesis of elements heavier than iron via the rapid neutron-capture (*r*) process has been the subject of intense studies since its mechanism was first proposed [1,2]. In recent decades, remarkable progress has been made on many fronts, including the advancement of astrophysical simulations, the detection of multimessenger events associated with gravitational waves, and observations of metal-poor stars in the Milky Way halo and in ultrafaint dwarf galaxies [3–5]. In these contexts, the second *r*-process abundance peak (with the mass number $A \sim 130$) plays a crucial role. Recent observations of Te in metal-poor stars by the Hubble Space Telescope [6–8] have shown that the peak is produced along with the rare-earth elements but with a larger variability across stars that is not yet fully understood [9,10]. This is possibly linked to the sensitivity of the peak to the *r*-process conditions or to contributions from other nucleosynthesis processes [11,12]. Observation of Te and Cs has been tentatively reported in the near-infrared during the kilonova event following neutron star merger GW170817 [13]. Conclusive data are likely to require future 30 m class telescopes [14] that may provide invaluable new information on the second *r*-process peak. Detection of other elements such as Sb, I, and Xe may also be possible [13]. In addition, the next generation of space observatories [15,16] may be able to detect γ rays from the radioactive decay of the peak's progenitors [17].

To connect the growing body of observations to astrophysics models and ultimately derive the *r*-process conditions, knowledge of the properties of the second *r*-process peak radioactive progenitors is essential. The peak has long been associated with the reduced neutron capture cross sections of nuclei with neutron number $N = 82$, which would cause such isotones to build up. The *r*-process matter flow would then break out of the $N = 82$ shell below atomic number $Z = 50$. Here, the nucleosynthesis path involves unstable nuclei which decay by β-delayed neutron emission (βn)—a process where, due to the large β-decay Q values, neutron-unbound states are populated in the daughter nuclei. Following the exhaustion of free neutrons, the *r*-process freezes out, and the second peak originates from a complex network of competing reactions including βn, neutron captures, and photodisintegration reactions. Depending on the neutron richness of the astrophysical environment, fission of heavy nuclei near the end point of the *r* process ($A > 260$) will also contribute to the second peak [18–20].

In this Letter, we report measurements of β-decay half-lives and β-delayed one- and two-neutron emission

probabilities (P_{1n} and P_{2n}) south-east of ^{132}Sn, reaching the edge of *r*-process paths predicted by several *r*-process models [21,22]. P_{xn} in this region are key to model accurately the $A \sim 130$ peak. Theoretical P_{xn} value predictions show large discrepancies [23,24], and their reliability is limited by the strong sensitivity to experimentally unknown nuclear structure details such as masses, neutron separation energies, β-decay strength distributions, and densities of states. In addition, near the *r*-process path, β-delayed multineutron emission channels are expected, with competition between different channels posing an additional modeling challenge. Relevant to the *r*-process nucleosynthesis ($Z > 28$), only six strong $\beta 2n$ emitters ($P_{2n} > 1\%$) have been measured to date [25–28], and only one of them (^{134}In) lies south-east of ^{132}Sn [27]. Our data provide new experimental inputs for *r*-process calculations and a new testing ground for models required to predict P_{xn} of *r*-process nuclei unreachable today.

Neutron-rich nuclei were produced by in-flight fission of an ~ 50 pnA, 345 MeV/nucleon ^{238}U beam impinging on a 4 mm Be target. Fission fragments were separated using the BigRIPS separator [29] and identified on an event-by-event basis using energy loss, time-of-flight, and magnetic rigidity information [30] before being implanted into the stack of six highly segmented silicon detectors of the Advanced Implantation Detector Array (AIDA) [31]. Figure 1 shows a particle identification plot of the implanted ions.

AIDA was surrounded by two clover-type HPGe detectors [32] and the BRIKEN neutron detector consisting of 140 ^{3}He proportional counters embedded in a high-density polyethylene moderator [33,34]. The neutron detection
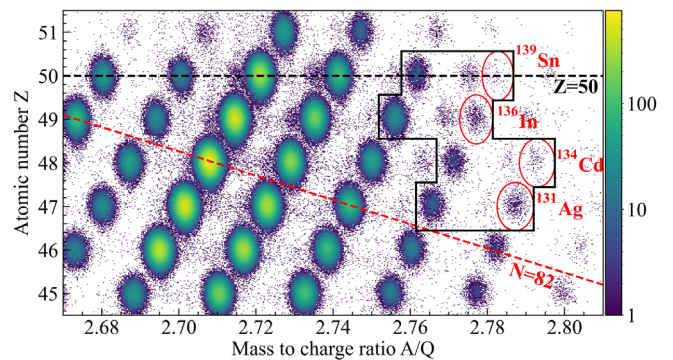

FIG. 1. Particle identification plot of ions implanted in AIDA. The black contour highlights the isotopes with P_n measured for the first time in this Letter. The heaviest isotope reported in this Letter is labeled for each element.

efficiency was carefully modeled using GEANT4 Monte Carlo simulations [34] and validated by measurements of a ^{252}Cf neutron source [35]. It is nearly constant up to 1 MeV with an average value of 66.8(20)%, dropping to about 59% at 3 MeV [33,36]. The systematic uncertainty introduced by the unknown neutron spectra was estimated as in Ref. [37]. Signals from all our detectors were recorded by digital acquisition systems synchronized with BigRIPS [31,38].

Implanted ions were correlated with electrons from subsequent β decays on the basis of detection time and position in the silicon detectors [39]. Neutrons were correlated with β decays within a 400 μs time window, needed to account for the neutron thermalization. The unbinned distribution of time differences between implantations and correlated β decays with their associated neutron multiplicity was fitted using the maximum likelihood method to determine simultaneously half-lives and P_{xn} values. The fits employ probability density functions that include a parent, all daughter's activities, and neutron background and consider the β and neutron efficiency of the detector setup [33,40,41].

The P_{1n} and P_{2n} measured in this Letter are reported in Table I. They are in good agreement with the literature values for In isotopes, but large differences were found for ^{131,132}Cd and ^{136,137}Sn [42,43], also in the half-lives. Half-lives from this Letter are generally consistent with the previous measurements performed at RIBF [39,44], although differences for ^{130}Cd, ^{131,132}In, and ^{134,136}Sn of $\lesssim 10\%$ are not fully understood. The reason for these differences can be related to the employed β-counting systems.

P_{xn} systematics are shown in Fig. 2, where an abrupt increase of the P_{1n} at $N = 84$ is observed for Cd, In, and Sn isotopes. Such an increase of P_{1n} clearly correlates with the sudden drop of neutron separation energy S_n in daughter nuclei beyond the $N = 82$ shell gap. The relatively small P_{1n} of Sn isotopes reflects the small Q_β of these isotopes relative to their lighter isotopes. This is due to the $Z = 50$ proton shell closure. For Ag isotopes, a large P_{1n} value increase occurs at $N = 83$ (^{130}Ag) rather than $N = 84$. This behavior departs from the systematic trend highlighted above and is somewhat unexpected considering that S_n in the daughter nucleus ^{130}Cd is rather large [6.06(2) MeV [50]]. Further investigation, e.g., via neutron spectroscopy, is needed to explain this behavior.

Our P_{1n} and P_{2n} were compared with the predictions of two theoretical models, the quasiparticle random-phase approximation (QRPA) [52,53] based on the microscopic-macroscopic finite range droplet model (FRDM) [54] and the relativistic Hartree-Bogoliubov (RHB) plus proton-neutron QRPA (pnQRPA) [55]. The latest versions of these models incorporate the treatment of the β-delayed emission phase under the framework of the Hauser-Feshbach (HF) statistical model with nominal level densities [56–59]. We find that, for the In isotopes, the inclusion of HF vastly improves model predictions that would otherwise grossly overestimate the P_{2n}/P_{1n} ratios. However, for FRDM + QRPA + HF this is true only up to ^{135}In; the large drop for theoretical P_{1n} in ^{136}In is not observed experimentally. The reason for this is unclear; the attempt to tune the level density of ^{135}Sn was not sufficient, as it showed that a modification of a few orders of magnitude would be required to match our data. The inclusion of the HF model improves to some extent the predictions for Cd isotopes, but the calculations still fail to reproduce the experimental values, while in Ag isotopes the inclusion of HF worsens the predictions. In the case of the

TABLE I. β-decay half-lives, P_{1n} and P_{2n} measured in this Letter and reported in the literature. Literature half-lives are from Lorusso et al. [44] unless stated otherwise. The nuclei with a possible mixture of β decays from ground and millisecond isomeric states are tagged with an asterisk (*).

Nuclide	$T_{1/2}^{\text{exp}}$ [ms]	$T_{1/2}^{\text{lit}}$ [ms]	P_{1n} [%]	P_{2n} [%]	P_{1n} lit [%]	Nuclide	$T_{1/2}^{\text{exp}}$ [ms]	$T_{1/2}^{\text{lit}}$ [ms]	P_{1n} [%]	P_{2n} [%]	P_{1n} lit [%]
^{129}Ag*	53.6(13)	52(4)	$18.6^{+1.7}_{-0.9}$	< 1.2	17.9(14) [23]	^{133}In*	166(4)	163(7)	89(5)	< 1.2	90(3)% [45]a
^{130}Ag	44(3)	42(5)	66(6)	< 5	...	^{134}In b	127(2)	126(7)	86^{+2}_{-4}	$11.9^{+1.2}_{-0.8}$	89(3) [27]
^{131}Ag	35(5)	35(8)	100^{+0}_{-6}	< 6	...	^{135}In	104(4)	103(5)	88^{+2}_{-5}	9.3(1.3)	...
^{130}Cd	135(2)	127(2)	2.9(2)	0	3.0(2) [23]	^{136}In	90(10)	85^{+10}_{-8}	84(10)	13(5)	...
^{131}Cd	100(2)	68(3) [42] 98.0(2)	$13.5^{+1.1}_{-0.7}$	< 0.7	3.5(1) [42]	^{134}Sn	1019(34)	890(20)	24.1(15)	0	17(13) [46]
^{132}Cd	82.5(9)	97(10) [42] 82(4)	100^{+0}_{-6}	< 1.7	60(15) [42]	^{135}Sn	514(30)	515(5)	20(2)	< 2.5	21(3) [47]
^{133}Cd	61(6)	64(8)	86(7)	6(2)	...	^{136}Sn	366(5)	300(15) [43] 350(5)	$18.5^{+2.4}_{-1.3}$	< 0.37	27(4) [43]
^{134}Cd	38(31)	65(15)	65(26)	< 39	...	^{137}Sn	231(7)	273(7) [43] 230(30)	23(2)	0.45(24)	50(10) [43]
^{131}In*	278(7)	261(3)	2.9(3)	0	2.3(3) [48]c	^{138}Sn	150(21)	140^{+30}_{-20}	28(5)	1.8(13)	...
^{132}In	214(8)	198(2)	12.2(12)	< 1.6	12.3(4) [49]	^{139}Sn	139(61)	130(60)	56(34)	< 86	...

aFor the $9/2^+$ ground state. $P_{1n} = 93(3)\%$ for the $1/2^-$ isomeric state [45].

b$P_{2n} = 9(2)\%$ [27].

cFor the combined $9/2^+$ ground state and $1/2^-$ isomeric state. $P_{1n} = 12(7)\%$ for the $21/2^+$ isomeric state [48].
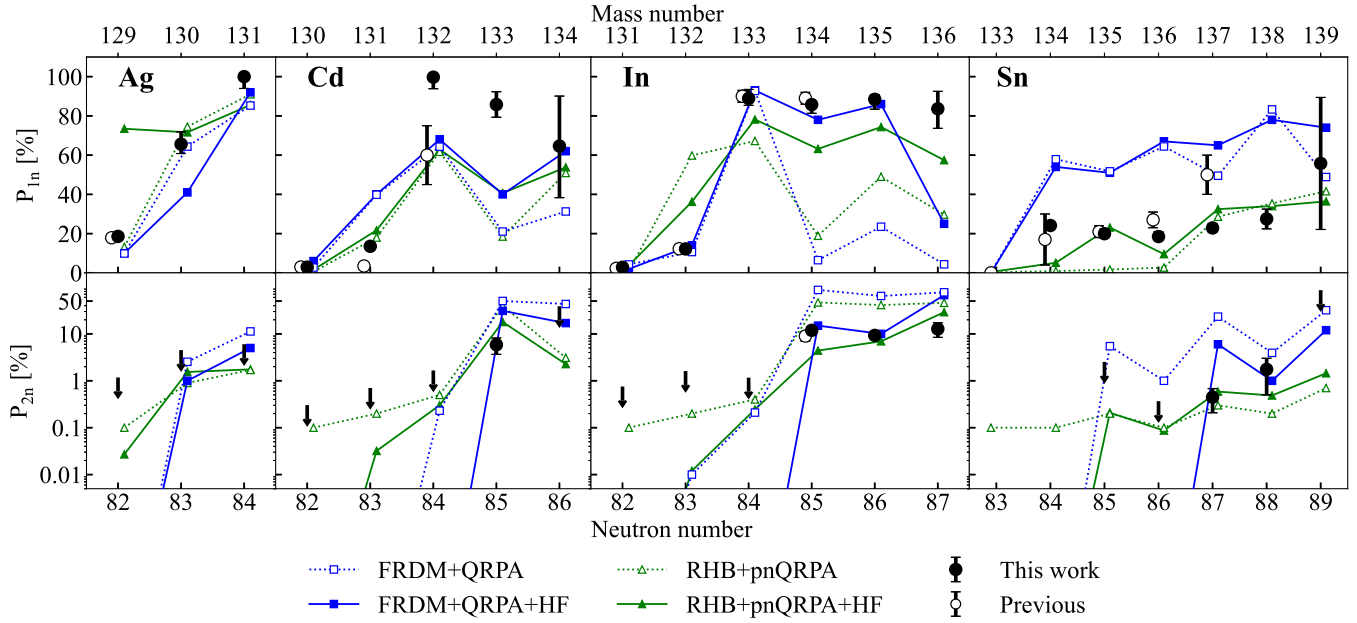
FIG. 2.   Systematics of measured P_{1n} and P_{2n} compared with literature values [23,27,42,43,45–49,51] and theoretical calculations.

Sn isotopes, FRDM + QRPA systematically overestimates P_{1n} by nearly a factor of 3. RHB + pnQRPA + HF performs better; however, it systematically underestimates half-lives by about a factor of 5 and underestimates P_n values for $N < 82$. Therefore, in the following r-process calculations, we use both models.

To understand the role of the measured P_{xn} and their impact in the astrophysical r process, we have carried out reaction network calculations using the SkyNet [60] and Nucnet [61] codes with reaction rates from the JINA REACLIB V2.2 database [62]. β-decay rates were updated with the P_{xn} values and half-lives from this Letter; neutron-induced and spontaneous fission was considered as in Ref. [63]. We chose r-process conditions compatible with merging neutron stars [64] with entropy $S^b = 12 k_B/\text{baryon}$, electron fraction $Y_e^b = 0.062$, and expansion timescale $\tau^b = 66$ ms. These conditions (baseline calculation) were found to best reproduce the Solar System abundance in the mass range $A = 129–139$, which is the one most affected by our P_n values.

The nuclear reaction flow during freeze-out for the baseline calculation is shown in Fig. 3(a). One notices that the progenitors for the elements of the second peak are all βn emitters (produced by either neutron capture or fission). Many such progenitors are included in our measurements, and some of their P_{xn} values are critical to determine the pathway to stability of neutron-rich material. For example, the abundance of ^{130}Te is produced predominantly by a βn flow from ^{131}Ag, the P_n value of ^{129}Ag affects the flow to ^{128}Te, and ^{132}Xe receives a large contribution from the βn of ^{134}Cd and ^{133}In. ^{133}Cs is critically affected by the βn flows from ^{134}In, ^{135}In, and

^{134}Cd. The P_{xn} values for these isotopes are now experimentally known. Among the isotopes affected by our data, ^{128,130}Te, ^{133}Cs, and ^{136}Xe are particularly important, because they are exclusively produced in the r process, so their abundance uncertainty is small.

To quantify the impact of our experimental P_{xn} values on the final abundances, we compared the abundances produced by our baseline simulation to those of three other calculations where the P_{xn} values of interest are set to the values predicted by the FRDM + QRPA + HF, RHB + pnQRPA + HF models, and the effective density model (EDM). The latter is a phenomenological multiple-neutron emission model based on a level density function with parameters empirically determined from existing experimental data [66]. The resulting final abundances and their corresponding changes relative to the baseline calculation are shown in Figs. 3(b) and 3(c). Differences of up to 30% are found when using the theoretical P_n values. The shadowed area provides an estimate of the r-process calculation uncertainty removed by our measurement. Notably, when FRDM + QRPA + HF values are used, the odd-even staggering beyond mass $A = 132$ is less pronounced. This is mainly due to the model overestimation of P_{1n} values for Sn isotopes (see Fig. 2). The calculations above were repeated over the large parameter space $Y_e = 0.005–0.062$ suitable to produce nuclei in the mass range $A = 129–139$. In this Y_e range, the r-process abundance pattern is formed robustly and the odd-even pattern does not change; hence, we consider our conclusion on the role of our measurements robust.

The impact of the new measurements on the odd-even abundance pattern can also be tested against Ba
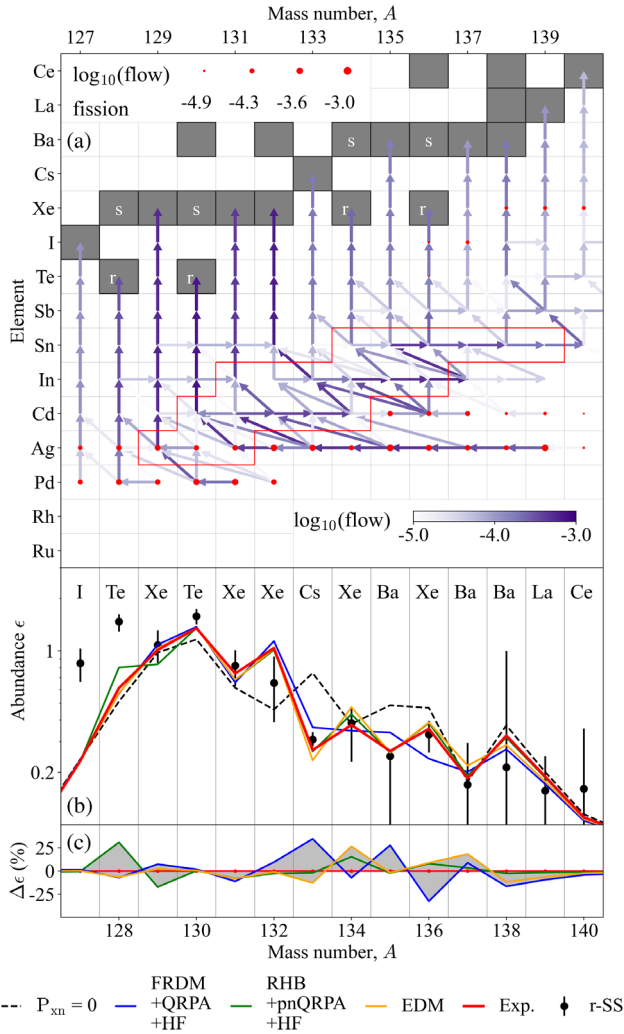
FIG. 3. (a) Time-integrated reaction flows during r-process freeze-out. The flows from fission reactions are marked with solid red circles with size proportional to their strength. The flows of other reactions and β decays are indicated by arrows weighted by their strength. The enclosed red line indicates the nuclear region of interest in this Letter. Stable isotopes are indicated as gray-filled squares, with those produced only by the slow neutron-capture process and the r process are tagged as "s" and "r," respectively. (b) Calculated r-process abundances using P_{1n} and P_{2n} from this Letter and from theoretical models (solid lines). A calculation with $P_{xn} = 0$ (black dash) is reported to identify the abundances most affected by βn. Solar abundances [65] are shown as black circles. (c) Abundance changes $\Delta\epsilon$ (in percent) for different models relative to the baseline calculation and combined as gray bands.

observations in r-process-enhanced metal-poor stars. Differences in the hyperfine structure splitting among Ba isotopes allow the determination of odd-mass Ba isotope abundances relative to the total Ba abundance ($f_{odd,Ba}$) [67]. $f_{odd,Ba}$ is an important indicator of isotopic composition, useful in characterizing the relative contribution of r- and s-process abundances. Figure 4 shows the $f_{odd,Ba}$ measured in five r-II stars with a strongly enhanced r process [68]
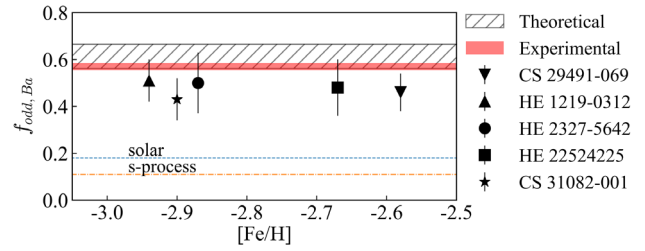
FIG. 4. Odd-mass Ba isotopic fraction $f_{odd,Ba}$ for five r-process-enhanced stars (r-II) labeled with their names [68,69] compared to $f_{odd,Ba}$ calculated using experimental P_{xn} (red band) and a range of $f_{odd,Ba}$ calculated using P_{xn} predicted by the three models considered in this Letter (shaded area), with FRDM + QRPA + HF resulting in the upper limit and RHB + pnQRPA + HF in the lower one. $f_{odd,Ba}$ for solar (dashed line) and pure s-process (dash-dotted line) abundances [70]. The metallicity [Fe/H] is defined as the logarithm of the iron-to-hydrogen number density ratio normalized to that of the sun.

along with the value calculated using experimental P_{xn} (red band). The figure also shows the range of $f_{odd,Ba}$ calculated using P_{xn} predicted by the three models considered in this Letter (shaded band). The comparison illustrates that the use of experimental P_{xn} leads to a more accurate odd-even abundance reducing the uncertainty in r-process calculations. Note that $f_{odd,Ba}$ in the Solar System has a large uncertainty due to s-process contaminants, especially in ^{138}Ba. The Ba abundance in metal-poor stars is, therefore, an important complementary test of the odd-even pattern in this mass range.

In summary, we have carried out the measurement of 20 β-delayed neutron emission probabilities for isotopes of Ag, Cd, In, and Sn beyond the $N = 82$ shell closure, reporting eight new P_{1n}, five new P_{2n}, and P_{2n} upper limits for all 20 of the nuclei studied. The new measurements provide a new picture of P_n systematics crossing the $N = 82$ and $Z = 50$ shells that includes for the first time Ag and extends significantly our knowledge of Cd, In, and Sn. Our P_n for ^{131,132}Cd and ^{136,137}Sn are at variance with previous data. The new measurements provide a new experimental ground to test nuclear models, with P_{2n} being particularly important to test the Hauser-Feshbach model of competition between β-delayed emission channels. Disagreements with theoretical models highlight the importance of experimental measurements. The new data have a direct impact on r-process calculations, removing up to nearly 30% of uncertainty deriving from theoretical models and improving the agreement with both the Solar System and metal-poor r-process-enhanced star abundances. This is an important new step forward toward a more reliable description of the second abundance peak and of key elements such as Te, Cs, and Ba. Isotopes with two neutrons beyond the limit of this experiment are the next milestone for the study of P_{xn} in this region, likely to

complete the set of P_{xn} needed to model the second r-process peak. The observation of isotopes with β_{3n} emission is also of great interest.

---

[*]phong@ribf.riken.jp
[†]nishimu@ribf.riken.jp

[1] F. Hoyle, W. A. Fowler, G. R. Burbidge, and E. M. Burbidge, Science **124**, 611 (1956).
[2] E. M. Burbidge, G. R. Burbidge, W. A. Fowler, and F. Hoyle, Rev. Mod. Phys. **29**, 547 (1957).
[3] C. Sneden, J. J. Cowan, and R. Gallino, Annu. Rev. Astron. Astrophys. **46**, 241 (2008).
[4] John J. Cowan, Christopher Sneden, James E. Lawler, Ani Aprahamian, Michael Wiescher, Karlheinz Langanke, Gabriel Martínez-Pinedo, and Friedrich-Karl Thielemann, Rev. Mod. Phys. **93**, 015002 (2021).
[5] T. Kajino, W. Aoki, A. B. Balantekin, R. Diehl, M. A. Famiano, and G. J. Mathews, Prog. Part. Nucl. Phys. **107**, 109 (2019).
[6] I. U. Roederer and J. E. Lawler, Astrophys. J. **750**, 76 (2012).
[7] Ian U. Roederer, James E. Lawler, John J. Cowan, Timothy C. Beers, Anna Frebel, Inese I. Ivans, Hendrik Schatz, Jennifer S. Sobeck, and Christopher Sneden, Astrophys. J. **747**, L8 (2012).
[8] Ian U. Roederer, James E. Lawler, Jennifer S. Sobeck, Timothy C. Beers, John J. Cowan, Anna Frebel, Inese I. Ivans, Hendrik Schatz, Christopher Sneden, and Ian B. Thompson, Astrophys. J. Suppl. Ser. **203**, 27 (2012).
[9] I. U. Roederer *et al.*, Astrophys. J. Suppl. Ser. **260**, 27 (2022).
[10] I. U. Roederer *et al.*, Astrophys. J. **936**, 84 (2022).
[11] Y.-Z. Qian and G. Wasserburg, Phys. Rep. **333–334**, 77 (2000).
[12] F. Montes, T. C. Beers, J. Cowan, T. Elliot, K. Farouqi, R. Gallino, M. Heil, K.-L. Kratz, B. Pfeiffer, M. Pignatari, and H. Schatz, Astrophys. J. **671**, 1685 (2007).
[13] S. J. Smartt *et al.*, Nature (London) **551**, 75 (2017).
[14] TMT project, https://www.tmt.org.
[15] V. Tatischeff *et al.*, in *Space Telescopes and Instrumentation 2016: Ultraviolet to Gamma Ray*, Vol. 9905, International Society for Optics and Photonics (SPIE, Bellingham, WA, 2016), pp. 843–853.
[16] R. Rando, J. Instrum. **12**, C11024 (2017).
[17] M.-H. Chen, L.-X. Li, D.-B. Lin, and E.-W. Liang, Astrophys. J. **919**, 59 (2021).
[18] M. Eichler *et al.*, Astrophys. J. **808**, 30 (2015).
[19] J.-F. Lemaître, S. Goriely, A. Bauswein, and H.-T. Janka, Phys. Rev. C **103**, 025806 (2021).
[20] T. M. Sprouse, M. R. Mumpower, and R. Surman, Phys. Rev. C **104**, 015803 (2021).
[21] S. Shibagaki, T. Kajino, G. J. Mathews, S. Chiba, S. Nishimura, and G. Lorusso, Astrophys. J. **816**, 79 (2016).
[22] M. R. Mumpower, R. Surman, G. McLaughlin, and A. Aprahamian, Prog. Part. Nucl. Phys. **86**, 86 (2016).
[23] O. Hall *et al.*, Phys. Lett. B **816**, 136266 (2021).
[24] P. Dimitriou *et al.*, Nucl. Data Sheets **173**, 144 (2021).
[25] K. Miernik *et al.*, Phys. Rev. Lett. **111**, 132502 (2013).
[26] R. Yokoyama *et al.*, Phys. Rev. C **100**, 031302(R) (2019).
[27] M. Piersa-Siłkowska *et al.* (IDS Collaboration), Phys. Rev. C **104**, 044328 (2021).
[28] B. Moon *et al.*, Phys. Rev. C **95**, 044322 (2017).
[29] T. Kubo *et al.*, Prog. Theor. Exp. Phys. **2012**, 03C003 (2012).
[30] N. Fukuda, T. Kubo, T. Ohnishi, N. Inabe, H. Takeda, D. Kameda, and H. Suzuki, Nucl. Instrum. Methods Phys. Res., Sect. B **317**, 323 (2013).
[31] C. J. Griffin *et al.*, in *Proceedings of the 14th International Symposium on Nuclei in the Cosmos (NIC2016), JPS Conference Proceedings* (2017), Vol. 14, p. 020622, 10.7566/JPSCP.14.020622.
[32] V. H. Phong *et al.*, Phys. Rev. C **100**, 011302 (2019).

[33] A. Tolosa-Delgado *et al.*, Nucl. Instrum. Methods Phys. Res., Sect. A **925**, 133 (2019).

[34] A. Tarifeño-Saldivia *et al.*, J. Instrum. **12**, P04006 (2017).

[35] M. Pallas *et al.*, arXiv:2204.13379.

[36] M. Pallas, A. Tarifeno-Saldivia *et al.* (to be published).

[37] A. Tolosa-Delgado, Study of beta-delayed neutron emitters in the region of ^{78}Ni and its impact on *r*-process nucleosynthesis, Ph.D. thesis, 2020, https://roderic.uv.es/handle/10550/76149.

[38] J. Agramunt *et al.*, Nucl. Instrum. Methods Phys. Res., Sect. A **807**, 69 (2016).

[39] O. Hall *et al.*, RIKEN Accel. Prog. Rep. **52**, 38 (2019), https://www.nishina.riken.jp/researcher/APR/APR052/pdf/38.pdf.

[40] V. H. Phong, S. Nishimura, and L. H. Khiem, Commun. Phys. **28**, 311 (2018).

[41] B. Rasco *et al.*, Nucl. Instrum. Methods Phys. Res., Sect. A **911**, 79 (2018).

[42] M. Hannawald *et al.* (ISOLDE Collaboration), Phys. Rev. C **62**, 054301 (2000).

[43] O. Arndt *et al.*, Phys. Rev. C **84**, 061307(R) (2011).

[44] G. Lorusso *et al.*, Phys. Rev. Lett. **114**, 192501 (2015).

[45] J. Benito *et al.* (IDS Collaboration), Phys. Rev. C **102**, 014328 (2020).

[46] M. Asghar, J. P. Gautheron, G. Bailleul, J. P. Bocquet, J. Greif, H. Schrader, G. Siegert, C. Ristori, J. Crancon, and G. I. Crawford, Nucl. Phys. **A247**, 359 (1975).

[47] J. Shergur *et al.*, Phys. Rev. C **65**, 034313 (2002).

[48] R. Dunlop *et al.*, Phys. Rev. C **99**, 045805 (2019).

[49] K. Whitmore *et al.*, Phys. Rev. C **102**, 024327 (2020).

[50] M. Wang, W. J. Huang, F. G. Kondev, G. Audi, and S. Naimi, Chin. Phys. C **45**, 030003 (2021).

[51] G. Rudstam, K. Aleklett, and L. Sihver, At. Data Nucl. Data Tables **53**, 1 (1993).

[52] P. Möller, B. Pfeiffer, and K.-L. Kratz, Phys. Rev. C **67**, 055802 (2003).

[53] P. Möller, M. R. Mumpower, T. Kawano, and W. D. Myers, At. Data Nucl. Data Tables **125**, 1 (2019).

[54] P. Möller, A. J. Sierk, T. Ichikawa, and H. Sagawa, At. Data Nucl. Data Tables **109–110**, 1 (2016).

[55] T. Marketin, L. Huther, and G. Martínez-Pinedo, Phys. Rev. C **93**, 025805 (2016).

[56] T. Kawano, P. Möller, and W. B. Wilson, Phys. Rev. C **78**, 054601 (2008).

[57] T. Kawano, P. Talou, M. B. Chadwick, and T. Watanabe, J. Nucl. Sci. Technol. **47**, 462 (2010).

[58] M. R. Mumpower, T. Kawano, and P. Möller, Phys. Rev. C **94**, 064317 (2016).

[59] F. Minato, T. Marketin, and N. Paar, Phys. Rev. C **104**, 044321 (2021).

[60] J. Lippuner and L. F. Roberts, Astrophys. J. Suppl. Ser. **233**, 18 (2017).

[61] B. S. Meyer and D. C. Adams, Meteorit. Planet. Sci. Suppl. **42**, 5215 (2007), https://journals.uair.arizona.edu/index.php/maps/article/download/15476/15464.

[62] R. H. Cyburt *et al.*, Astrophys. J. Suppl. Ser. **189**, 240 (2010).

[63] J. Lippuner and L. F. Roberts, Astrophys. J. **815**, 82 (2015).

[64] S. Fujibayashi, S. Wanajo, K. Kiuchi, K. Kyutoku, Y. Sekiguchi, and M. Shibata, Astrophys. J. **901**, 122 (2020).

[65] S. Goriely, Astron. Astrophys. **342**, 881 (1999), https://adsabs.harvard.edu/pdf/1999A%26A...342..881G.

[66] K. Miernik, Phys. Rev. C **90**, 054306 (2014).

[67] P. Magain and G. Zhao, Astron. Astrophys. **268**, L27 (1993), https://hdl.handle.net/2268/21071.

[68] C. Wenyuan, J. Xiaohua, S. Jianrong, Z. Gang, and Z. Bo, Astrophys. J. **854**, 131 (2018).

[69] X. Y. Meng, W. Y. Cui, J. R. Shi, X. H. Jiang, G. Zhao, B. Zhang, and J. Li, Astron. Astrophys. **593**, A62 (2016).

[70] Claudio Arlandini, Franz Kappeler, Klaus Wisshak, Roberto Gallino, Maria Lugaro, Maurizio Busso, and Oscar Straniero, Astrophys. J. **525**, 886 (1999).

Correction: Minor errors in values given in the fourth row of the eleventh column and first footnote of Table I have been fixed.